

COMMON ORIGIN OF BLACK HOLES IN HIGH MASS X-RAY BINARIES AND IN GRAVITATIONAL-WAVE SOURCES

K. BELCZYNSKI¹, C. DONE², S. HAGEN², J.-P. LASOTA^{1,3}, K. SEN⁴

¹ Nicolaus Copernicus Astronomical Center, Polish Academy of Sciences, ul. Bartycka 18, 00-716 Warsaw, Poland
(chrisbelczynski@gmail.com)

² Department of Physics, University of Durham, South Road, Durham DH1 3LE, UK

³ Institut d'Astrophysique de Paris, CNRS et Sorbonne Université, UMR 7095, 98bis Bd Arago, 75014 Paris, France

⁴ Institute of Astronomy, Faculty of Physics, Astronomy and Informatics, Nicolaus Copernicus University, Grudziądzka 5, PL-87-100 Toruń, Poland

Draft version October 10, 2023

ABSTRACT

Black hole (BH) high mass X-ray binary (HMXB) systems are likely the progenitors of the BH-BH mergers detected in gravitational waves by LIGO/Virgo/KAGRA (LVK). Yet BHs in the gravitational wave sources reach higher masses ($\sim 100 M_\odot$) than BHs in HMXBs ($\sim 20 M_\odot$), and have typically lower spins ($a_{\text{BH}} \lesssim 0.25$ with tail extending to larger values) than the published values for BHs in HMXBs ($a_{\text{BH}} \gtrsim 0.9$). This could suggest that these two classes of systems belong to different populations (“apples and oranges”) but we show here that it does not have to be the case. The difference in masses is easily explained as the known HMXB-BHs are in galaxies with relatively high-metallicity, so their progenitor stars are subject to strong mass loss from winds which leads to relatively low mass BH at core collapse. Conversely, LVK allows for detection of BHs from low-metallicity galaxies that naturally produce more massive stellar-origin BHs. The explanation of the difference in BH spins is not as straightforward, but we show that in HMXBs the BH spin-value derivation depends strongly on how the HMXB accretion disk emission is modeled. We demonstrate this explicitly for the case of Cyg X-1, showing excellent spectral fits with low spin ($a_{\text{BH}} \sim 0.1$) when taking into account the Comptonization of the disk photosphere. Similar results have recently been shown for LMC X-1 (allowing for $a_{\text{BH}} \sim 0.1$). We suggest that such low BH spins are generic for all three HMXB BHs. Hence we conclude that current observations are consistent with LVK BHs and HMXB BHs belonging to the same population (“all apples”).

Subject headings: stars: black holes, compact objects, massive stars

1. INTRODUCTION

LIGO/Virgo/KAGRA (LVK) interferometers have detected gravitational waves from 70 double black hole (BH-BH) mergers (The LIGO Scientific Collaboration et al. 2023). These merging black holes (BHs) have masses in range $\sim 3\text{--}100 M_\odot$, with many primary (more massive) BHs having masses of $\sim 10 M_\odot$ and $\sim 35 M_\odot$. The most massive LVK event (GW190521) showed two merging BHs with estimated mass of $\sim 95 M_\odot$ and $\sim 69 M_\odot$. The majority of these mergers have low positive effective spin parameters, with the distribution that peaks at

$$\chi_{\text{eff}} = \frac{m_1 a_{\text{BH},1} \cos \theta_1 + m_2 a_{\text{BH},2} \cos \theta_2}{m_1 + m_2} \approx 0.05, \quad (1)$$

where m_i denotes BH masses, $a_{\text{BH},i} = cJ_i/Gm_i^2$ are BH spin magnitudes (J_i : BH angular momentum (AM), c , G : the speed of light and the gravitational constant), and θ_i are angles between the system’s angular momentum and BH spins. Out of these 70 mergers 6 show high positive effective spins $\chi_{\text{eff}} > 0.3$ (mean), while none show high negative spin $\chi_{\text{eff}} < -0.3$. However, there are 3 events with moderate negative spin estimates:

$-0.3 < \chi_{\text{eff}} < -0.1$. Low values of the effective spin parameter may result from small individual BH spin magnitudes (Belczynski et al. 2020). This finds support in LVK data that shows that BH individual spin magnitudes in BH-BH mergers peak at $a_{\text{BH}} \sim 0.1\text{--}0.2$, although distribution has a long tail; that extends to large values (The LIGO Scientific Collaboration et al. 2023).

Electromagnetic observations have revealed a population of BHs hosted in binary star systems (e.g., see <https://universeathome.pl/universe/blackholes.php> and references therein). Out of several known binary configurations hosting BHs, only high-mass X-ray binaries (HMXBs) can potentially lead to BH-BH mergers, as BH companion stars are massive enough to form a BH. Three BH HMXBs have such massive ($\gtrsim 20 M_\odot$) companions: LMC X-1 ($\sim 30 M_\odot$), Cyg X-1 ($\sim 40 M_\odot$), and M33 X-7 ($\sim 70 M_\odot$). BHs observed in these HMXBs have moderate masses: $10.9 M_\odot$ for LMC X-1, $15.7 M_\odot$ for M33 X-7, and $21.2 M_\odot$ for Cyg X-1 (Miller-Jones et al. 2021b). Spins of BHs in HMXBs are obtained with three methods (disk continuum fitting, reflection spectroscopy, and reverberation) and estimated spin values are generally high: $a_{\text{BH}} = 0.84$ for M33 X-7, $a_{\text{BH}} = 0.92$ for LMC X-1, and $a_{\text{BH}} > 0.9$ for

Cygnus X-1 (see Tab.1 in Fishbach & Kalogera 2022).

Since the spins and, to some extent, masses of LVK BHs and HMXB BHs appear to be different, it may seem that these two groups indicate populations with different formation scenarios. Here, we show how all these BHs may instead form one single population. The difference in BH mass arises naturally from the diverse formation environments: all known HMXB-BH are in local group galaxies with relatively high metallicity, so there are strong stellar winds before core collapse, resulting in lower black hole masses compared to those forming in low metallicity galaxies which are within the sensitivity range of LVK. We demonstrate the difference in expected black hole masses explicitly using a population synthesis model. This model also reproduces the spin values seen in the LVK BHs, where high spin is only produced by tidal spin up in extremely close binaries. None of the known HMXB-BH systems are in binary systems which are close enough for this, so should not have high spins, in conflict with reported values. Here we demonstrate that these high spin values are model dependent even for the well known and well studied Cyg X-1 system (see also Zdziarski et al. (2023a) for a similar analysis of LMC X-1). Therefore, there is no requirement for a conflict in spin, allowing the BHs in BH-BH mergers and the HMXBs to form from the same population.

2. BH MASSES

To demonstrate the unicity of the BH population, we use the population synthesis code **StarTrack** (Belczynski et al. 2002, 2008) and employ the delayed core-collapse supernova (SN) engine for neutron star/BH mass calculation (Fryer et al. 2012) that does not produce a lower mass gap between NSs and BHs. We use a model with metallicity-dependent BH mass spectrum (Belczynski et al. 2010a; Fryer et al. 2012) updated here to produce BHs as massive as $20 M_{\odot}$ at high metallicity (e.g., formation of Cyg X-1 in Milky Way) and allowing for the formation of BHs as massive as $M_{\text{BH}} = 90 M_{\odot}$ at low metallicity (e.g., GW190521 LVK merger detected at distance of ~ 4 Gpc Abbott et al. (2020)).

In Figure 1 we show the dependence of the Helium core mass on metallicity for single stars obtained with the stellar wind treatment presented in Belczynski et al. (2010a). The helium core mass is a good approximation of the BH mass since binary interactions (Roche Lobe Overflow or common envelope evolution) tend to remove the H-rich envelope from stars in close binaries (progenitors of BH-BH mergers if these form through isolated binary evolution). The lower the metallicity, the lower opacity in stellar atmospheres and the lower wind mass loss produces progressively higher mass BHs with decreasing metallicity.

Cyg X-1 is located in the Milky Way disk that hosts stars with about solar metallicity ($Z = 0.014$ Asplund et al. (2009)). For such metallicity, we obtain a maximum BH mass of $M_{\text{BH}} \sim 20 M_{\odot}$, which is consistent with the highest mass stellar-origin BH known in Milky Way for the same Cyg X-1 ($M_{\text{BH}} = 21 M_{\odot}$ Miller-Jones et al. (2021b)). LMC X-1 is located in the Large Magellanic Cloud ($Z \approx 0.005$) and M33 X-7 in M33 galaxy ($Z = 0.01$). In this metallicity range, BHs are not expected to be more massive than $M_{\text{BH}} \sim 35 M_{\odot}$.

The LVK BH-BH mergers have already been detected

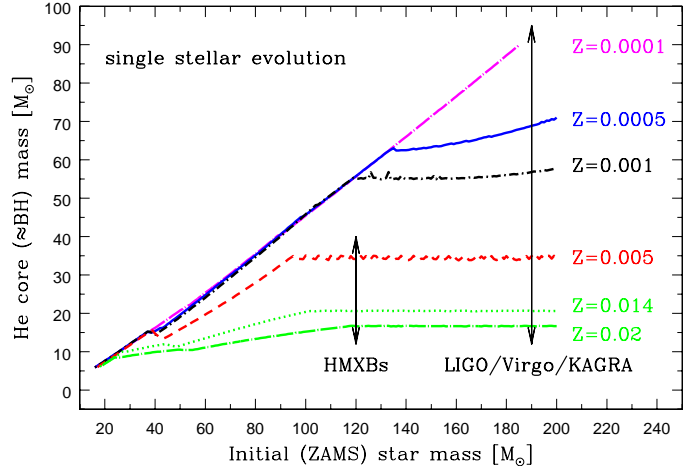


FIG. 1.— The helium core mass is a function of the initial star mass for various metallicities. The helium core is a good approximation of the black hole mass for stars in close binaries that form BH-BH mergers (Binary interactions remove h-rich envelope). Black arrows show the current stellar metallicity range of LVK (low-redshift Universe: $z < 0.7$) and for HMXBs that are limited to the local group of galaxies. LVK is bound to probe more massive BHs than electromagnetic HMXB observations.

(O3) to significant redshifts of $z \lesssim 0.7$. The detected BH-BH mergers may have formed even at much larger redshifts due to non-zero delay time between star formation and BH-BH mergers (Dominik et al. 2012; Fishbach & Kalogera 2021). Therefore, galaxies and stars that can produce BH-BH mergers cover a wide range of metallicity. It is even claimed that Population III (metal-free) stars ($Z = 0$) can contribute to LVK detections (Kinugawa et al. 2014). Assuming a metallicity range $Z = 0.0001 - 0.02$ for LVK we obtain a broad range of BH mass: $\sim 3 - 90 M_{\odot}$. This range is consistent with the LVK BH mass estimates in BH-BH mergers.

In conclusion, the same model of stellar evolution produces correct mass ranges for the three discussed HMXB BHs (narrow) and LVK BHs (wide).

3. BH SPINS: POPULATION SYNTHESIS

The population synthesis model can also be used to predict the BH spin distribution. It employs the standard Tayler-Spruit magnetic dynamo for angular momentum transport that produces low-spinning BHs ($a_{\text{BH}} \sim 0.1$) from non-interacting stars and low- to rapidly-spinning BHs ($a_{\text{BH}} = 0.1 - 1.0$) for Wolf-Rayet (WR) stars that were subject to tidal spin-up in close binaries (Belczynski et al. 2020; Bavera et al. 2020). This model can explain low and high effective spins of LVK BH-BH mergers (Olejak & Belczynski 2021).

However, this scenario predicts that the HMXB-BH should be formed with low spins ($a_{\text{BH}} \sim 0.1$). Accretion from wind (even when they are L1-focused) from the companions in Cyg X-1, M33 X-7, and LMC X-1 cannot increase significantly BH spins in these systems while the orbital periods of these systems are too large for tidal interactions to spin up the stars before they form BHs. Therefore applying this model to HMXBs implies that their BH spins are low, with $a \lesssim 0.4$ – consistent with LVK BH spins (Fishbach & Kalogera 2022), but clearly incompatible with the reported spin values in these systems. To solve this apparent inconsistency we

re-examine below the methods of determining BH spins in HMXBs.

4. BH SPINS: HMXBS

The main tracer of BH spin in the electromagnetic systems is the radius of the innermost stable circular orbit (R_{ISCO}). This sets the inner inner radius of the accretion disk in the standard Shakura-Sunyaev (Shakura & Sunyaev 1973 and its relativistic extension: Novikov-Thorne; Novikov & Thorne 1973) models. Measuring the inner edge of the disk gives an estimate of BH spin, with R_{ISCO} decreasing from $6 - 1.23R_g$ (R_g being the gravitational radius of a BH) as a_{BH} increases from $0 - 1$. The most direct way to do this uses the luminosity emitted by the accretion disk itself (we review other methods in the discussion).

Standard accretion disk models balance gravitational heating from viscous torques with blackbody cooling, resulting in an optically thick, geometrically thin structure with temperature at each radius, $T^4(R) \propto (L/R^2)(R_{\text{ISCO}}/R)$. This gives a total spectrum which is a sum over all radii of blackbody spectra of different temperatures. The emissivity peaks around $R \sim R_{\text{ISCO}}$, so the peak temperature is $\propto (L/R_{\text{ISCO}}^2)^{1/4}$ K, i.e. is a factor $2.2\times$ higher for the same disk luminosity at high spin than at low spin.

There is more complexity: the emission does not quite thermalize (often approximated by a color temperature correction) and the emitted light is subject to special and general relativistic effects as it propagates out to the observer. These effects can all be calculated, and are routinely included in the fits. More problematic is that there is generally a power-law tail in the spectrum extending to much higher energies, clearly showing that there is an additional non-disk component to the accretion flow. Nevertheless, picking spectra where this is small means the underlying accretion disk assumption is likely to be reliable (see Appendix 8.1 for more details).

Instead, the issue we highlight below is that the strong soft component need not be emitted by a simple blackbody disk, where the energy is dissipated mainly on the midplane, but can have heating further up into the photosphere. This forms a warm layer on the top of the disk, making it appear hotter and hence giving higher spin when fit with standard disk models. Such a warm layer on the disk is sometimes required in the black hole binaries (e.g. in very high/intermediate type spectra: Kubota et al. 2001; Remillard & McClintock 2006) and is generic in Active Galactic Nuclei (Porquet et al. 2019; Gierliński & Done 2004; Petrucci et al. 2018).

We demonstrate the effect of a warm skin on the disk on derived BH spin below using Cyg X-1.

5. CYG X-1 SPIN FROM THE SOFT COMPONENT

We use data from the softest ever state seen, where the soft component is at its most dominant and so uncertainties from modeling the high energy coronal tail are smallest (observation B4 from Kawano et al. 2017, see this paper for details of the data). We fit these data using the XSPEC spectral fitting package and all the models below include absorption along the line of sight using TBABS with column density as a free parameter. We show results from a series of model fits in Figure 2, where the

original (absorbed) X-ray Suzaku data is grey, with the reconstructed (corrected for absorption) spectrum shown with orange points. We assume here the standard mass and distance, and fix the disk inclination to the binary inclination of $i = 30^\circ$. Details of the fitting are described in Appendix 8.2.

We first fit the standard disk model to these data. The results are shown in the left panel of Figure 2. This includes all special and general relativistic ray tracing effects, as well as allowing a correction to the blackbody temperatures to account for the incomplete thermalisation expected from full models of the vertical disk structure (color temperature correction, fixed to 1.7). We allow a fraction of these disk spectra to be Compton up-scattered to form the power law tail, modelled using the standard formalism which assumes the electron energy is typically higher than 100 keV. We recover the standard, very high black hole spin ($a_{\text{BH}} = 0.96$) seen in all literature fits to the soft component.

The middle panel of Figure 2 shows what happens when we additionally allow a warm skin on the top of the disk. We model this using another Compton upscattering model which allows the electron temperature to be a free parameter, as well as the scattered fraction (set by the optical depth of the skin). This is formally a much better fit to the data, even accounting for the 2 additional free parameters (optical depth and temperature of the warm disk skin). More importantly here, the best fit reduces BH spin to $a_{\text{BH}} = 0.77$, and this is extremely poorly constrained as the soft component shape is now set more by the electron temperature of the skin than by the temperature of the disk at the ISCO. We illustrate this in the right panel of Figure 2, where we show a fit with almost the same χ^2_ν but for $a_{\text{BH}} = 0.1$ as expected from the Taylor-Spruit dynamo used above.

This demonstrates that formal solutions for BH spins from spectra with their reported extremely small error bars or very definitive values (e.g., $a_{\text{BH}} > 0.9985$ at 3σ level (Zhao et al. 2021b)) are model-dependent and are not necessarily the only solution. This is especially the case as recent polarization measurements may indicate a higher inclination for the inner accretion flow in Cyg X-1 ($i = 45 - 65^\circ$ Krawczynski et al. 2022). We show in Appendix 8.3 how a higher inclination gives lower BH spin both for the standard disk and warm skin models.

6. DISCUSSION

Using Cyg X-1 we demonstrated that the disk spectrum fitting method to measure BH spin is not necessarily secure. The soft component in LMC X-1 can also be fit with similar models of a warm skin over the disk, again resulting in much lower spin being consistent with the data (Zdziarski et al. 2023a). However, there are alternative ways to measure BH spin, so we discuss below the constraints these give for the BHs in HMXBs.

6.1. Alternative measures of BH spin

The X-ray tail shows that some part of the accretion energy is emitted outside of the optically thick disk structure. As such it will illuminate the disk. Some fraction of this will reflect from free electrons in the disk, while some is absorbed by inner shell electrons, ejecting them from the atom/ion. The most prominent line is from iron

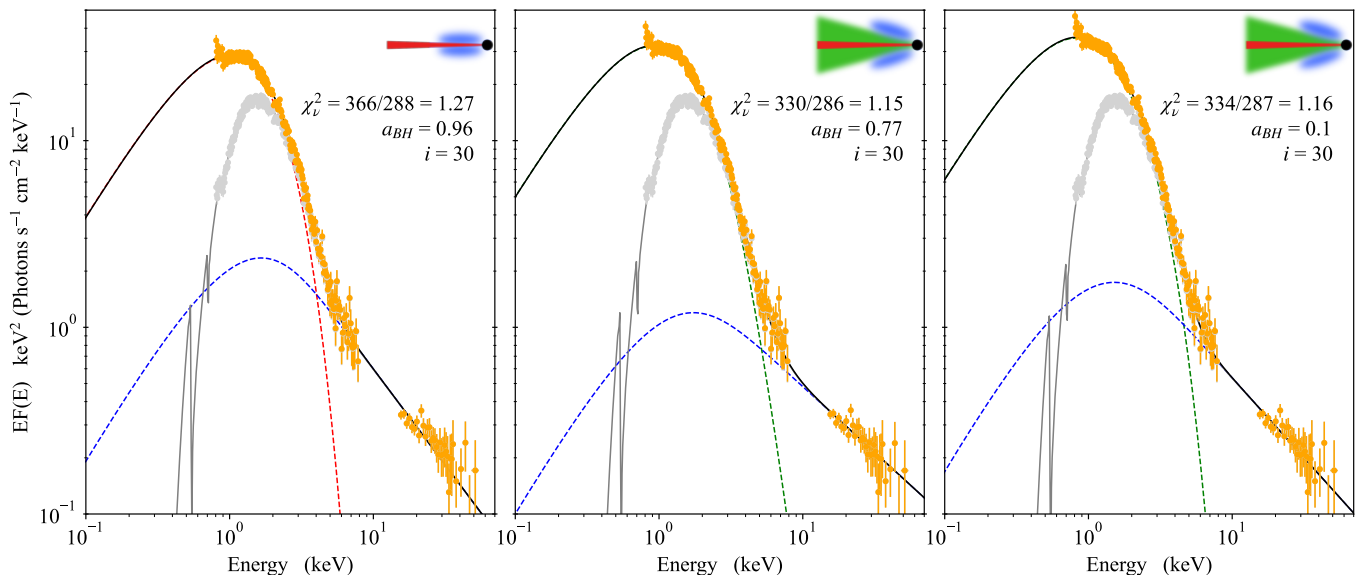


FIG. 2.— Cyg X-1 spectra for for: *Left*: A standard accretion disk (red), modeled with KERRBB, and a hot Comptonizing plasma (blue) giving the high energy emission - as sketched in the top right corner; model (a). *Middle*: A standard accretion disk entirely covered by a warm Comptonizing plasma (green), and then an inner hot Comptonizing plasma (blue); model (b). *Right*: Same as middle, but with the spin fixed at $a_{\text{BH}} = 0.1$. Note that the low BH spin is fully consistent with the X-ray spectral data.

K α , and in the simplest models where the disk is neutral, this line is intrinsically narrow, at rest frame energy of 6.4 keV. Special and general relativistic effects (Doppler red/blue shifts, transverse and gravitational redshifts) broaden the observed line, so its profile directly depends on how much of the line arises from each radius of the disk. Hence this allows estimates of BH spin (Fabian et al. 1989; García et al. 2014). This is very simple and physically compelling, but in reality there is more complexity.

Firstly this broadened line is not a large feature, typically contributing only maximum $\sim 5 - 10\%$ above the continuum. This is why disk continuum fitting for black hole spin should be more robust, as long as the standard disk does dominate the observed emission.

The smaller the inner disk radius, the broader the line but this makes it harder to distinguish it from the continuum. The tracer of extreme spin is the extent of the extreme red wing of the iron line, which is very difficult to decompose uniquely, especially as the illuminating continuum shape is unlikely to be a single Comptonization component.

Secondly, the disk is not neutral. There is a range of ionization states present in BH accretion disks so the emitted lines are between 6.4 – 7 keV rather than at a fixed energy and the intrinsic line profile depends on the detailed radial and vertical ionization structure of the material. Relativistic broadening is then a further distortion on an already broad feature (see e.g. Basak & Zdziarski 2016).

In Cyg X-1 there are multiple reflection fits which derive high spin assuming a single Comptonization component (e.g. $a_{\text{BH}} > 0.9$; Duro et al. 2016), but assuming a more complex continuum (which is strongly favored by the data) removes all constraints on spin (Basak et al. 2017). There are many fewer results for LMC X-1 as

the source is much less bright, and the tail is less strong, making these features harder to determine but there are similar uncertainties (see Zdziarski et al. (2023a) versus Steiner et al. (2012)).

There is a long running, controversial discussion in the accreting Low-mass X-ray binary (LMXB) BH community on how to measure BH spin. The LMXBs do show spectra which look very like standard disks, but these can give BH spin which are in conflict with the reflection spins. A recent, very well-studied example is MAXI J1820+070, a low-mass X-ray transient with a $M \sim 8.5 M_{\odot}$ BH and a $\sim 0.6 M_{\odot}$ companion (Torres et al. 2020). On the one hand, using continuum fitting, Zhao et al. (2021a) and Guan et al. (2021) find for the BH in this source $a_{\text{BH}} = 0.14$ and $a_{\text{BH}} = 0.2$. Fitting reflection spectra can give extreme spin (Buisson et al. 2019) or no constraints at all (Zdziarski et al. 2021), depending on the continuum used.

Given the controversy over how to measure BH spin in accreting BHs, it seems premature to adopt the high spin values in HMXBs as reliable.

6.2. Can disk form in Cyg X-1 for low BH spin?

Our modelling of the disk continuum spectra assumes that an accretion disk can form around the BH for any value of the BH spin and/or any orientation of the accretion disk with respect to the spin of the BH. Sen et al. (2021) showed that, assuming spherically symmetric Bondi-Hoyle accretion (Bondi 1952), the formation of an accretion disk is sensitively dependent on the assumption of the spin of the BH and the orientation of the accretion disk with respect to the spin of the BH. For the observed binary and stellar parameters of Cyg X-1 (Miller-Jones et al. 2021a), a maximally spinning BH may be required to form an accretion disk in the prograde orientation.

However, we note that the O star companion in Cyg X-1 is nearly filling its Roche lobe (Roche-lobe filling factor is greater than 0.9 Miller-Jones et al. 2021a), where the formation of a focused accretion stream is expected (Blondin et al. 1991; Hadrava & Čechura 2012; El Mellah et al. 2019). In Cyg X-1, the existence of a focused accretion stream has also been observationally verified (Miller et al. 2005; Poutanen et al. 2008; Hanke et al. 2009). High Roche lobe filling factors have been found for the two other BH HMXBs, LMC X-1 (Orosz et al. 2009) and M33 X-7 (Orosz et al. 2007) as well.

In such a configuration, spherically symmetric Bondi-Hoyle accretion is not accurate. The tidal and gravitational effects of the BH distort the shape of the O star and wind streamlines from the O star, respectively (El Mellah et al. 2019; Hirai & Mandel 2021). Hirai & Mandel (2021) showed that for Cyg X-1, the effects of rotation and gravity darkening can lead to the formation of a prograde accretion disk around a non-rotating BH when the Roche lobe filling factor of the O star is greater than ~ 0.8 .

Hence, the criterion of the formation of an accretion disk in Cyg X-1 does not rule out any assumptions on the spin of the BH. The high Roche lobe filling factor of the O star enables the formation of a focused wind with sufficient angular momentum to make a prograde accretion disk.

The above arguments, together with our modelling of the disk continuum spectra imply that the observations of Cyg X-1 are consistent with the statement that its BH can also be slowly spinning.

7. CONCLUSION

The difference between HMXB and LVK BH masses has already been noticed after the first gravitational wave detection and attributed to metallicity effect (Abbott et al. 2016) as anticipated by Belczynski et al. (2010b). Taking into account that interferometric detectors of gravitational waves sample a volume that is a few hundred thousand times larger than the X-ray telescopes (for HMXB BH mass determination), the difference in BH masses between LVK and HMXBs is not surprising as it implies a huge difference in the metallicity range sampled (see Fig. 1).

While assessing the problem of BH mass difference between HMXB and gravitational-wave sources is rather straightforward, addressing that of the apparent conflicting spin values is more complicated. At face value, the spin values attributed to the BH in the HMXBs that are massive enough to form LVK sources (Cyg X-1, LMC X-1, M33 X-7) seem to require two distinct populations: slowly spinning (LVK) and rapidly spinning (HMXBs) BHs.

Since the majority of LVK BHs are slowly spinning

($a \sim 0.1 - 0.2$), we argue, under the assumption that they are stellar-origin BHs (i.e., are not primordial BHs: Hawking (1971)), that it must indicate that massive stars are subject to efficient angular momentum transport (Spruit 1999; Fuller et al. 2019). This leads to good agreement of predicted BH spins in BH-BH mergers with LVK data (Belczynski et al. 2020; Bavera et al. 2020). These slowly spinning BHs can form in isolated binary evolution and various dense (open, globular, nuclear) cluster environments. A small fraction of LVK BHs may be moderately or even rapidly spinning (see the long tail of BH spins with $a \gtrsim 0.4$: left panel of Fig.15 in The LIGO Scientific Collaboration et al. 2023). These moderately/rapidly spinning BHs can also be explained in the framework of efficient angular momentum transport. Although the star rotation slows down during its evolution towards the formation of a BH, the tidal spin-up of a WR star (BH progenitor) in close BH+WR binary systems (BH-BH progenitors) can easily result in a moderately or rapidly spinning BH (Olejak & Belczynski 2021). In dense clusters, dynamical interactions may lead to the formation of BH-BH mergers with components that are second or even third-generation BHs (formed by earlier BH-BH mergers) that naturally have significant spins (Rodríguez et al. 2019).

Under the natural assumption that BHs in HMXBs are formed directly from massive stars and within the paradigm of efficient angular momentum transport, these BHs must have low spins ($a \sim 0.1$; e.g., Belczynski et al. 2020). We have demonstrated that the most reliable and often used method of BH spin estimate based on fitting the disk spectra in HMXBs can be overestimated if there is a warm skin on top of the disk. In particular, we show that with this model the most observed system, Cyg X-1, can be consistent with slowly a spinning BH. The same warm skin solutions also give low spin for LMC X-1 (Zdziarski et al 2023) and almost certainly can fit to the much worse quality data from M33 X-7. We speculate that this warm skin is needed in the HMXB-BH due to the stellar wind Roche Lobe Overflow.

Thus we conclude that the LVK and HMXB BHs are consistent with having the same origin, i.e. with the LVC BHs forming directly from stars under the assumption of efficient angular momentum transport.

We would like to thank Jerome Orosz, Henric Krawczynski, Andrew King, and Andrzej Zdziarski for very useful comments on this study. KB acknowledges support from the Polish National Science Center (NCN) grant Maestro (2018/30/A/ST9/00050). CD acknowledges support from STFC through grant ST/P000541/1. SH acknowledges support from STFC through the studentship grant ST/V506643/1. KS is funded by the National Science Center (NCN), Poland, under grant number OPUS 2021/41/B/ST9/00757.

REFERENCES

- Abbott, B. P., et al. 2016, *ApJ*, 818, L22
 Abbott, R., et al. 2020, *Phys. Rev. Lett.*, 125, 101102
 Arnaud, K. A. 1996, in *Astronomical Society of the Pacific Conference Series*, Vol. 101, *Astronomical Data Analysis Software and Systems V*, ed. G. H. Jacoby & J. Barnes, 17
 Asplund, M., Grevesse, N., Sauval, A. J., & Scott, P. 2009, *ARA&A*, 47, 481
 Bardeen, J. M., & Petterson, J. A. 1975, *ApJ*, 195, L65
 Basak, R., & Zdziarski, A. A. 2016, *MNRAS*, 458, 2199
 Basak, R., Zdziarski, A. A., Parker, M., & Islam, N. 2017, *MNRAS*, 472, 4220
 Bavera, S. S., et al. 2020, *A&A*, 635, A97
 Belczynski, K., Bulik, T., Fryer, C. L., Ruiter, A., Valsecchi, F., Vink, J. S., & Hurley, J. R. 2010a, *ApJ*, 714, 1217
 Belczynski, K., Dominik, M., Bulik, T., O’Shaughnessy, R., Fryer, C. L., & Holz, D. E. 2010b, *ApJ*, 715, L138

- Belczynski, K., Kalogera, V., & Bulik, T. 2002, *ApJ*, 572, 407
- Belczynski, K., Kalogera, V., Rasio, F. A., Taam, R. E., Zezas, A., Bulik, T., Maccarone, T. J., & Ivanova, N. 2008, *ApJS*, 174, 223
- Belczynski, K., et al. 2020, *A&A*, 636, A104
- Belloni, T. M. 2010, *States and Transitions in Black Hole Binaries*, ed. T. Belloni, Vol. 794, 53
- Blondin, J. M., Stevens, I. R., & Kallman, T. R. 1991, *ApJ*, 371, 684
- Bondi, H. 1952, *MNRAS*, 112, 195
- Buisson, D. J. K., et al. 2019, *MNRAS*, 490, 1350
- Dexter, J., & Begelman, M. C. 2023, *arXiv e-prints*, arXiv:2308.01963
- Dominik, M., Belczynski, K., Fryer, C., Holz, D., Berti, B., Bulik, T., Mandel, I., & O’Shaughnessy, R. 2012, *ApJ*, 759, 52
- Duro, R., et al. 2016, *A&A*, 589, A14
- El Mellah, I., Sander, A. A. C., Sundqvist, J. O., & Keppens, R. 2019, *A&A*, 622, A189
- Fabian, A. C., Rees, M. J., Stella, L., & White, N. E. 1989, *MNRAS*, 238, 729
- Fishbach, M., & Kalogera, V. 2021, *ApJ*, 914, L30
- , 2022, *ApJ*, 929, L26
- Fryer, C. L., Belczynski, K., Wiktorowicz, G., Dominik, M., Kalogera, V., & Holz, D. E. 2012, *ApJ*, 749, 91
- Fuller, J., Piro, A. L., & Jermyn, A. S. 2019, *MNRAS*
- García, J., et al. 2014, *ApJ*, 782, 76
- Gierliński, M., & Done, C. 2004, *MNRAS*, 349, L7
- Gierliński, M., Zdziarski, A. A., Poutanen, J., Coppi, P. S., Ebisawa, K., & Johnson, W. N. 1999, *MNRAS*, 309, 496
- Gou, L., et al. 2009, *ApJ*, 701, 1076
- , 2011, *ApJ*, 742, 85
- Guan, J., et al. 2021, *MNRAS*, 504, 2168
- Hadrava, P., & Čechura, J. 2012, *A&A*, 542, A42
- Hanke, M., Wilms, J., Nowak, M. A., Pottschmidt, K., Schulz, N. S., & Lee, J. C. 2009, *ApJ*, 690, 330
- Hawking, S. 1971, *MNRAS*, 152, 75
- Heida, M., Jonker, P. G., Torres, M. A. P., & Chiavassa, A. 2017, *ApJ*, 846, 132
- Hirai, R., & Mandel, I. 2021, *PASA*, 38, e056
- Jana, A., & Chang, H.-K. 2023, *arXiv e-prints*, arXiv:2307.14604
- Kawamura, T., Done, C., Axelsson, M., & Takahashi, T. 2023, *MNRAS*, 519, 4434
- Kawano, T., Done, C., Yamada, S., Takahashi, H., Axelsson, M., & Fukazawa, Y. 2017, *PASJ*, 69, 36
- King, A. 2023, *Supermassive Black Holes*
- King, A., & Nixon, C. 2016, *MNRAS*, 462, 464
- , 2018, *ApJ*, 857, L7
- Kinugawa, T., Inayoshi, K., Hotokezaka, K., Nakauchi, D., & Nakamura, T. 2014, *MNRAS*, 442, 2963
- Krawczynski, H., Yuan, Y., Chen, A. Y., Rodriguez Cavero, N., Hu, K., Gau, E., Steiner, J. F., & Dovčiak, M. 2023, *arXiv e-prints*, arXiv:2307.13141
- Krawczynski, H., et al. 2022, *Science*, 378, 650
- Kubota, A., Makishima, K., & Ebisawa, K. 2001, *ApJ*, 560, L147
- Lasota, J.-P. 2001, *New Astronomy Reviews*, 45, 449
- Li, L.-X., Zimmerman, E. R., Narayan, R., & McClintock, J. E. 2005, *ApJS*, 157, 335
- Maccarone, T. J. 2002, *MNRAS*, 336, 1371
- Marcussen, M. L., & Albrecht, S. H. 2022, *ApJ*, 933, 227
- Martin, R. G., Tout, C. A., & Pringle, J. E. 2008, *MNRAS*, 387, 188
- Miller, J. M., Woźdowski, P., Schulz, N. S., Marshall, H. L., Fabian, A. C., Remillard, R. A., Wijnands, R., & Lewin, W. H. G. 2005, *ApJ*, 620, 398
- Miller-Jones, J. C. A., et al. 2021a, *arXiv e-prints*, arXiv:2102.09091
- , 2021b, *Science*, 371, 1046
- , 2021c, *Science*, 371, 1046
- Mirabel, I. F., & Rodrigues, I. 2003, *Science*, 300, 1119
- Novikov, I. D., & Thorne, K. S. 1973, in *Black Holes (Les Astres Occlus)*, 343–450
- Olejak, A., & Belczynski, K. 2021, *ApJ*, 921, L2
- Orosz, J. A., & Hauschildt, P. H. 2000, *A&A*, 364, 265
- Orosz, J. A., McClintock, J. E., Aufdenberg, J. P., Remillard, R. A., Reid, M. J., Narayan, R., & Gou, L. 2011, *ApJ*, 742, 84
- Orosz, J. A., et al. 2007, *Nature*, 449, 872
- , 2009, *ApJ*, 697, 573
- Paxton, B., et al. 2015, *ApJS*, 220, 15
- Petrucchi, P. O., Ursini, F., De Rosa, A., Bianchi, S., Cappi, M., Matt, G., Dadina, M., & Malzac, J. 2018, *A&A*, 611, A59
- Porquet, D., et al. 2019, *A&A*, 623, A11
- Poutanen, J., Veledina, A., & Beloborodov, A. M. 2023, *ApJ*, 949, L10
- Poutanen, J., Zdziarski, A. A., & Ibragimov, A. 2008, *MNRAS*, 389, 1427
- Poutanen, J., et al. 2022, *Science*, 375, 874
- Rao, A., Gandhi, P., Knigge, C., Paice, J. A., Leigh, N. W. C., & Bouber, D. 2020, *MNRAS*, 495, 1491
- Remillard, R. A., & McClintock, J. E. 2006, *ARA&A*, 44, 49
- Rodriguez, C. L., Zevin, M., Amaro-Seoane, P., Chatterjee, S., Kremer, K., Rasio, F. A., & Ye, C. S. 2019, *arXiv e-prints*, arXiv:1906.10260
- Schnittman, J. D., & Krolik, J. H. 2009, *ApJ*, 701, 1175
- , 2010, *ApJ*, 712, 908
- Sen, K., Xu, X. T., Langer, N., El Mellah, I., Schürmann, C., & Quast, M. 2021, *A&A*, 652, A138
- Shakura, N. I., & Sunyaev, R. A. 1973, *A&A*, 500, 33
- Spruit, H. C. 1999, *A&A*, 349, 189
- Steiner, J. F., Narayan, R., McClintock, J. E., & Ebisawa, K. 2009, *PASP*, 121, 1279
- Steiner, J. F., et al. 2012, *MNRAS*, 427, 2552
- Tauris, T. M. 2022, *ApJ*, 938, 66
- The LIGO Scientific Collaboration et al. 2023, *Physical Review X*, 13, 011048
- Torres, M. A. P., Casares, J., Jiménez-Ibarra, F., Álvarez-Hernández, A., Muñoz-Darias, T., Armas Padilla, M., Jonker, P. G., & Heida, M. 2020, *ApJ*, 893, L37
- Walton, D. J., et al. 2016, *ApJ*, 826, 87
- Weisskopf, M. C., et al. 2022, *Journal of Astronomical Telescopes, Instruments, and Systems*, 8, 026002
- Zdziarski, A. A., Banerjee, S., Chand, S., Dewangan, G., Misra, R., Szanecki, M., & Niedzwiecki, A. 2023a, *arXiv e-prints*, arXiv:2308.06167
- Zdziarski, A. A., Dzielak, M. A., De Marco, B., Szanecki, M., & Niedzwiecki, A. 2021, *ApJ*, 909, L9
- Zdziarski, A. A., Johnson, W. N., & Magdziarz, P. 1996, *MNRAS*, 283, 193
- Zdziarski, A. A., Szanecki, M., Poutanen, J., Gierliński, M., & Biernacki, P. 2020, *MNRAS*, 492, 5234
- Zdziarski, A. A., Veledina, A., Szanecki, M., Green, D. A., Bright, J. S., & Williams, D. R. A. 2023b, *ApJ*, 951, L45
- Zhao, X., et al. 2021a, *ApJ*, 916, 108
- , 2021b, *ApJ*, 908, 117
- , 2021c, *ApJ*, 908, 117

8. APPENDIX

8.1. *Disk continuum fitting and black hole spin*

Of the four known BH HMXBs, only LMC X-3 has a disk continuum spanning an extensive range of luminosity, giving a fairly robust and well-determined spin of $a_{\text{BH}} \sim 0.2$. Other HMXB-BHs have high mass transfer rates from high-mass companion stars, meaning that the disk is stable to the strong instability around hydrogen ionization temperatures, which produces the majority of variability, for example in LMXB-BHs (triggered at 5000 – 10,000 K: e.g. Lasota 2001). Therefore, other HMXB BH spins have been measured from fitting black body disk models to spectra around a single luminosity.

Changes in mass accretion rate onto the BH can result in dramatic spectral changes. Such systems go through a set of well-defined spectral states, so the same source transitions between a disk dominated state, so-called: “high/soft spectral state” (high luminosity, low energy photons dominating spectrum), and a hard X-ray corona-dominated state, so-called: “low/hard spectral state” (low luminosity, high energy photons being a significant part of the energy output of the accretion flow).

There is no consensus on the geometry and nature of the hot Comptonizing plasma. Suggestions include multiple parts of accretion flow: a non-thermalized disk, a corona above the disk, and/or a corona above/near the BH. All invoke magnetic fields, which may be dynamically important. Wherever it is, and however it is moving, it can illuminate a residual disk and produce a reflection and/or reprocessed signatures.

As well as these two main states, there are also transitional states which show much more complex spectral shapes which are even less well understood, making it even more difficult to derive black hole spin unambiguously. Below, we illustrate this in the famous HMXB binary Cyg X-1 case.

Cyg X-1 is a (quasi)-persistent source with a mass accretion rate that is fairly constant to within factors of $\sim 2 - 3$. However, this range includes the luminosity at which the accretion flow undergoes a dramatic transition, from emitting a soft spectrum, which looks something like a disk, to hard, where it looks nothing like a disk (e.g. Gierliński et al. 1999).

This (quasi)-persistent source has a mass accretion rate which is around the high/soft (disk-dominated) and low/hard (not disk-dominated) spectral transition so that the spectral shape can change quite dramatically for only a small change in bolometric luminosity (e.g. Gierliński et al. 1999). This means that Cyg X-1 does not go far from the transition from the high/soft (disk dominated) to the low/hard (not disk-dominated) state. It is unclear whether the source ever reaches a real disk-dominated state. Nonetheless, these softest spectra fit with standard disk spectra, and the resulting spins are extremely high ($a_{\text{BH}} > 0.95$: Gou et al. 2011; Walton et al. 2016; Zhao et al. 2021c).

We show clear evidence that the accretion flow *has not formed* a standard black body disk. Figure 3 shows the hardness-intensity diagram of the LMXB GX339-4. This source picks out a well-defined track, transitioning from low/hard (lower right) to disk-dominated (left), with fast transitions (horizontal) between the two states. The red points compare data from Cyg X-1 (both data taken from Belloni 2010). The mass and distance of GX339-4 are not well known, so we have scaled the relative count rate (brightness) between the two systems to match the lower transition luminosity. We can see how GX339-4 transitions from low/hard state (hardness ratio > 1 ; the ratio is defined as the ratio of counts in the energy bands 6.3–10.5 and 3.8–6.3 keV) to high/soft state (hardness ratio < 0.1). In contrast, Cyg X-1 never reaches as far to the left as seen in the GX339-4 disk-dominated states.

Cyg X-1 always has a stronger tail of emission to higher energies (e.g. Gierliński et al. 1999; Gou et al. 2009; Walton et al. 2016), making it appear stuck in the more complex intermediate states where it is not clear that the optically thick material thermalizes even to a color temperature-corrected blackbody. Instead, the soft component in intermediate state spectra is often better fit by optically thick, warm (few keV) Comptonization (see, for e.g. transition spectra from the LMXB-BH MAXI J1820+070 in Fig. 2 of Kawamura et al. 2023).

Cyg X-1 has a higher mass BH ($21.2 M_{\odot}$; Miller-Jones et al. 2021c) than GX339-4 ($\sim 2 - 10 M_{\odot}$; Heida et al. 2017), but this should make its disk spectra softer rather than harder since the ISCO is farther out for more massive BHs, making the disk temperature lower. A hotter disk temperature could instead result if Cyg X-1 has a substantially larger spin than GX339-4, but the reflection and reverberation spin estimates for GX339-4 are both extremely high.

Therefore, there is no evidence that a standard disk forms in the whole available set of observations of Cyg X-1. Suppose the inner disk has not yet fully collapsed into a standard disk. In that case, it will not completely thermalize, making this system’s standard disk-fitting method of BH spin determination inapplicable.

8.2. *Fitting Cyg X-1 spectra*

We fit Cyg X-1 using two models: one considering a standard disk, and another where the disk is covered by some warm optically thick material (model a and b respectively). In both cases we model the spectra using XSPEC v.12.13.0 (Arnaud 1996).

For the standard disk we use the XSPEC model KERRBB (Li et al. 2005). This considers multi-colour black-body emission originating from a disk structure, assuming Novikov & Thorne (1973) emissivity. All relativistic effects are taken into account, including ray-tracing from the disk to the observer. Additionally, this model always assumes that the disk extends to the ISCO.

However, Cyg X-1 always shows a high energy tail that cannot be disk emission. This is generally understood as originating from a hot optically thin inner corona, which Compton up-scatters incident disk photons to higher energies. To model this we convolve our disk emission, KERRBB, with SIMPL (Steiner et al. 2009). This takes an input seed spectrum (in this case KERRBB) and scatters a fraction of the seed photons into a power-law component (hence

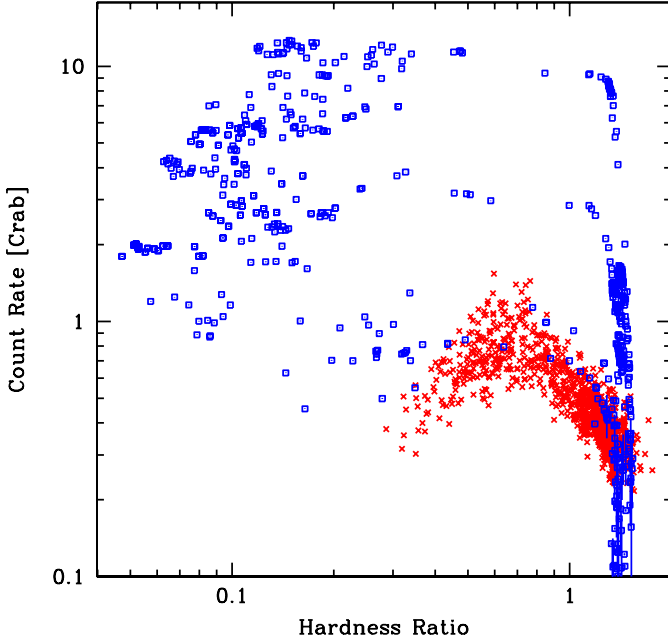


FIG. 3.— The spectral hardness versus intensity diagram for all the data from GX339-4 (blue) and Cyg X-1 (red), shifted in intensity so that the transition from soft to hard overlapped. Hardness ratio is defined as the ratio of counts in the energy bands 6.3–10.5 and 3.8–6.3 keV.

emulating a Comptonized spectrum). In XSPEC syntax, the model is `SIMPL*KERRBB`.

For model b we also have the addition of a warm optically thick skin covering the disk. This will also Compton up-scatter the disk photon to higher energies, but not sufficiently so to give a high energy tail. Instead this will give a spectrum that looks similar to a disk, but with the peak shifted to slightly higher energies and a shallower drop-off than the usual Wien tail. We model this using the convolution model `THCOMP` (Zdziarski et al. 1996, 2020). This takes an input seed spectrum and Compton scatters to higher energies, similar to `SIMPL`, however unlike `SIMPL` `THCOMP` takes the electron temperature of the Comptonizing plasma as an input argument, setting the high energy turn over. Additionally, for this optically thick skin we assume that all input seed photons are Compton scattered, unlike the case for the high-energy tail where only a fraction are scattered. In XSPEC syntax the model is now `CSIMPL*THCOMP*KERRBB`.

The line of sight absorption to Cyg X-1 is complex and variable. Hence we need to include an absorption component in both our models, for which we use `TBABS`. Due to the variable nature of the absorber in Cyg X-1 we leave the column-density in `TBABS` as a free parameter throughout. We note that in Figs 2, 4, and 6, we show the spectrum corrected for absorption in colour, and the original uncorrected spectrum in grey.

As the data originate from two different instruments, XIS (soft-xrays) and HXD (hard-xrays), though both onboard Suzaku, we include a cross-calibration constant in all our models. Throughout this is fixed to 1.15, i.e. increasing the model flux in the hard band by a factor 1.15. Finally, the total XSPEC models are: `CONST*TBABS*CSIMPL*KERRBB` for model a, and `CONST*TBABS*CSIMPL*THCOMP*KERRBB` for model b.

8.3. High inclination Cygnus X-1

Here, we use the same X-ray Cyg X-1 data and the same two BH accretion flow models as in Section 5. However, we allow inclination to change from the value obtained from the light curve and velocity curve analysis ($i \sim 30^\circ$).

In Figure 4 we show our best formal (in terms of χ^2_ν) fits for both models to the observational data. In both models, both BH spin and inclination were free parameters. For model (a) we find $a_{\text{BH}} = 0.8$ and $i = 43.5^\circ$, while for model (b) we find $a_{\text{BH}} = 0.45$ and $i = 51.1^\circ$. Note that both model match the data very well, although model (b) ($\chi^2_\nu = 1.15$) is a better fit than model (a) ($\chi^2_\nu = 1.26$).

In both fits, we obtain inclinations that are notably higher than measured from the light curve and velocity curve analysis and are typically adopted in other studies. In these fits, inclination is a free parameter not informed by other observations or analyses (i.e., without any imposed priors or biases). These high inclinations are favored by the data within the framework of these two very different accretion flow models.

Both BH spin estimates are significantly lower than results typically reported by other groups and lower than our corresponding results for the set inclination of $i = 30^\circ$ (compare with Fig. ?? left and middle panels). Such a result is explained by the anti-correlation between BH spin and inclination of the accretion flow.

In Figure 5, we demonstrate the anti-correlation between BH spin and inclination of the accretion flow in both of our adopted models. For both models, we note clear (different in details, but similar in general shape) trends: higher inclinations impose lower BH spins. The unfortunate fact is that by allowing for arbitrary inclination, we can find a very good match to the spectral X-ray data to almost any desired value of BH spin. This degeneracy between

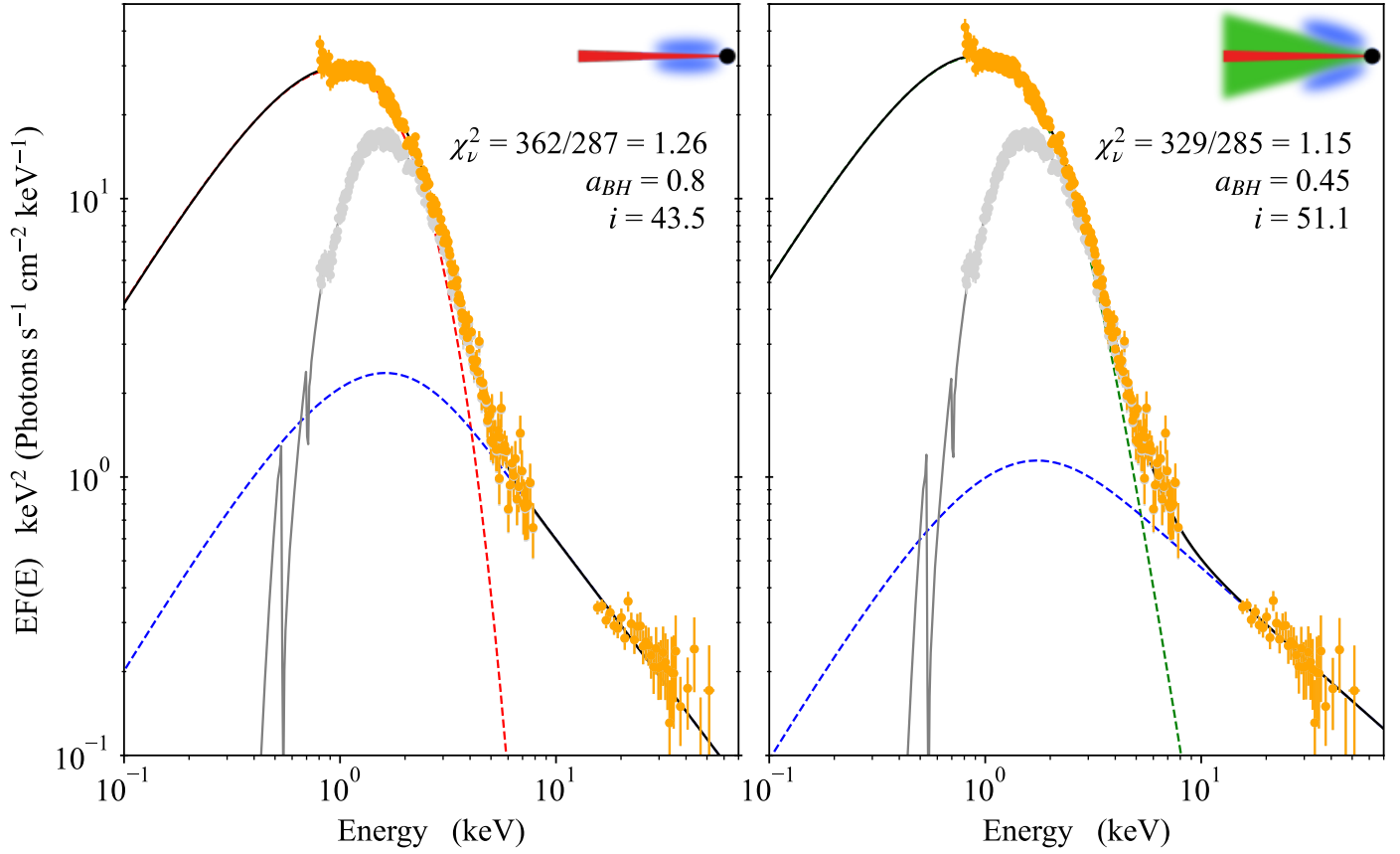


FIG. 4.— Cyg X-1 spectra fit for our two BH accretion models in which we fit simultaneously BH spin and inclination. Lines/points are the same as in Fig. 2. Note that these best formal fits to data move inclinations to higher values ($i \sim 40 - 50^\circ$) and BH spins to smaller values ($a_{\text{BH}} \sim 0.5 - 0.8$) as compared with the same models in which inclination was set to $i = 30^\circ$ giving BH spin of $a_{\text{BH}} \sim 0.8 - 1.0$ (see Fig 2 left and middle panels).

inclination and BH spin hinders the power of this type of analysis. Relativistic Doppler boosting increases with increasing inclination (the accretion flow is seen more edge-on), making the disk appear hotter/bluer. Decreasing BH spin can compensate for this, making ISCO larger and the disk appear cooler/redder. Therefore, similar solutions/fits can be found for pairs of anti-correlated inclinations—BH spins.

In Figure 6 we show three fits performed with model (b) with inclination set to $i = 30, 45, 60^\circ$ (not a free parameter anymore) and a BH spin a free parameter. All three fits match the data very well ($\chi^2_\nu = 1.15$ for all of them), but the model predicts very different values of BH spin: $a_{\text{BH}} = 0.77, 0.56, 0.25$ for increasing inclination, respectively. Not surprisingly, for low inclination of $i = 30^\circ$, similar to what was adopted in many previous studies, the BH spin is rather high $a_{\text{BH}} = 0.77$, but not extreme in this model. However, for higher inclinations, the BH spin decreases. In particular, for inclination of $i = 60^\circ$, the BH spin becomes small enough $a_{\text{BH}} = 0.25$ to be consistent with recent LVK measurements of BH spins in gravitational-wave data (half of BH spins are $a_{\text{BH}} \lesssim 0.25$).

8.3.1. Orbit vs Accretion Flow Inclination in Cyg X-1

The hottest and the innermost X-ray emitting region counts in most in the X-ray spectra fitting method to estimate BH spin (along with other parameters). In principle orbital inclination (i_{orb}) can be different from the inclination of the inner accretion flow (i_{xray} ; defined as the angle between the line of sight and the axis perpendicular to the inner accretion flow). So far in our analysis, we have assumed that both inclinations are the same ($i = i_{\text{orb}} = i_{\text{xray}}$). But this does not have to be true. And each model fitted to the BH X-ray spectrum employs i_{xray} and not i_{orb} .

Given the physical size of the orbit ($a = 52.5 R_\odot$ (Miller-Jones et al. 2021b)) and O-star ($R = 22.3 R_\odot$) eclipses the BH (and thus X-rays) for orbital inclinations of $i_{\text{orb}} > 67^\circ$. Since Cyg X-1 is not eclipsing, only smaller inclinations of the orbit are allowed. However, if the inner part of the disk is warped, its inclination (i_{xray}) may have an arbitrary value, and it will not cause any eclipses as long as the orbital plane inclination is $i_{\text{orb}} < 67^\circ$. The X-ray emitting region's physical size is very small compared to the orbit size. Depending on the accretion flow model, X-ray emitting region size found in our simulations in the range $\sim 200 - 1000 \text{ km}$ ($\sim 0.0003 - 0.0014 R_\odot$).

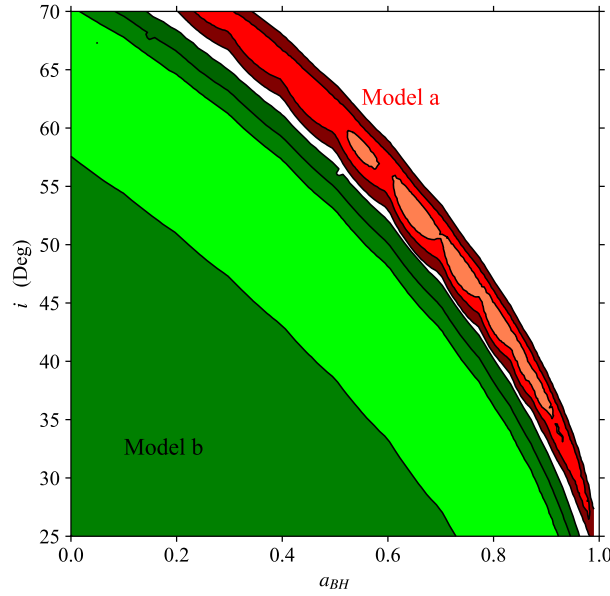


FIG. 5.— Contour plot of black hole spin versus inclination for the two spectral models considered in this paper: a standard accretion disk (red, model **(a)**) and a disk covered by a warm Comptonizing plasma (green, model **(b)**). The contours are drawn for $\Delta\chi^2 = 2.3, 6.17, 11.8$, corresponding to 1, 2, 3 σ confidence intervals for two varying parameters.

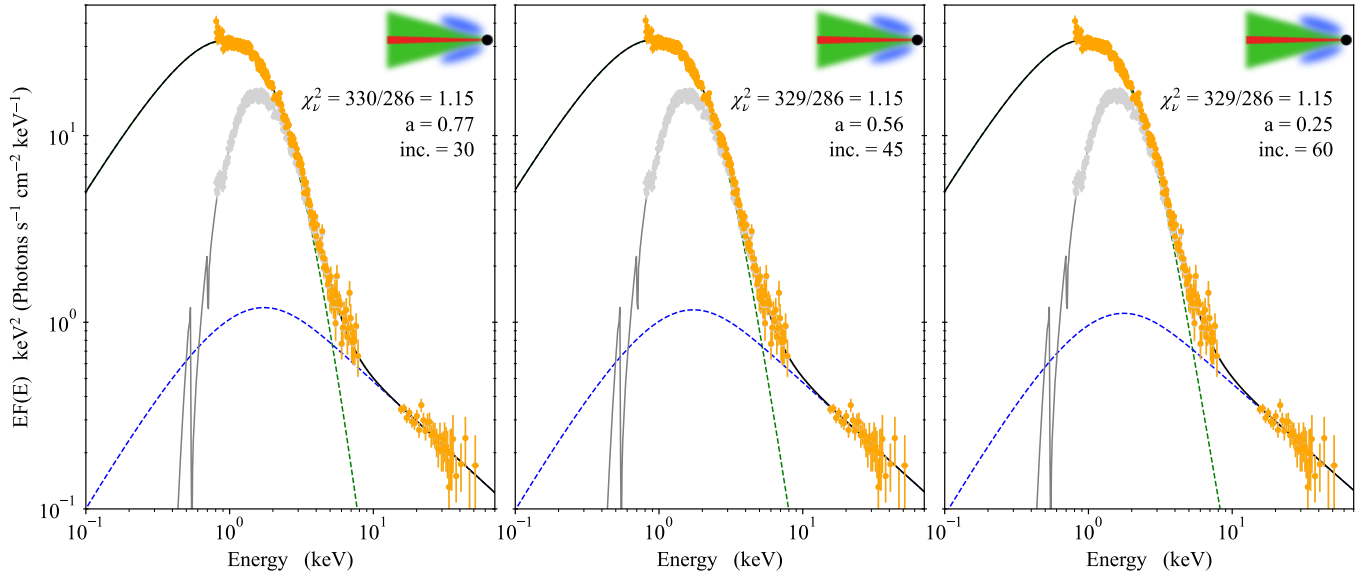


FIG. 6.— Cyg X-1 spectra for our choice of BH accretion model **(b)** for 3 adopted inclinations $i = 30, 45, 60^\circ$ (larger the inclination the disk is seen more edge-on). BH spin is a free parameter in each fit, and we present the best formal match to the data. Note that all fits give a ($\chi^2_\nu = 1.15$) similarly good match to the data. For the lowest inclination ($i = 30^\circ$) we estimate high (but not extreme) BH spin of $a_{\text{BH}} = 0.77$ (same fit as shown in Fig. ?? right panel). However, for higher inclinations, BH spin decreases. In particular, for $i = 60^\circ$, we measure low BH spin of $a_{\text{BH}} = 0.25$. This is consistent with recent LVK estimate of BH spins (half of BHs have low spins: $a \lesssim 0.25$).

Orosz et al. (2011) have performed Cyg X-1 light curve and radial velocity curve analysis to estimate system physical parameters. In particular, they have estimated system orbit inclination (defined as the angle between line-of-sight and binary angular momentum vector; $i_{\text{orb}} = 90^\circ$: orbit edge-on). Their preferred solution resulted in $i_{\text{orb}} = 27.1 \pm 0.8^\circ$. Despite the use of sophisticated methods (Orosz & Hauschildt 2000), the estimate of inclination is problematic, especially in the light that the system is not eclipsing and that the O star does not fill its Roche lobe (so it is not maximally geometrically distorted diminishing effects of inclination on light curve shape). Light curve solutions have

inherent degeneracies between inclination and limb darkening, mass ratio, and gravity darkening. This is reflected in a broad range of inclination values $i_{\text{orb}} \sim 26 - 68^\circ$ found by Orosz et al. (2011) in their various light curve/radial velocity curve solutions. Additionally to these uncertainties, it is crucial to note that these are estimates of the position of the orbital plane that are not informed in any way by the position of accretion flow/disk. This comes from the fact that O star greatly dominates in optical and UV light curves over emission from the accretion disk (which dominates in X-rays). Orosz et al. (2011) estimated that in optical O-star emission dominates by factor of $\sim 10,000$ over disk emission. Therefore, disk emission and its position/inclination play no role in their analysis. In other words, if the accretion flow were misaligned with the orbital plane, such analysis would not reveal this. More recent analysis of Miller-Jones et al. (2021c), who, with the revised Cyg X-1 distance and increased component masses, obtained orbital inclination of $i_{\text{orb}} = 27.51^\circ$.

The spatial position of accretion flow may be measured with the polarization of X-rays for a given accreting BH, both from thermalized (soft state) emission (Schnittman & Krolik 2009) as well as from coronal (hard state) emission (Schnittman & Krolik 2010). Two independent analyses of polarization observations of Cyg X-1 by the NASA Imaging X-ray Polarimetry Explorer (Weisskopf et al. 2022) resulted in measurement of high degree of polarization of $\sim 4\%$ and $\sim 2.7\%$ in soft and hard state, respectively (Krawczynski et al. 2022; Jana & Chang 2023). New observations of Cyg X-1 in hard state confirm previous measurements with an estimate of polarization at the level of $\sim 2.3\%$ (see The Astronomer’s Telegram at <https://www.astronomerstelegam.org/?read=16084>). The inclination of accretion flow inferred from these observations is $i_{\text{xray}} \sim 45 - 65^\circ$. High polarization degree favors higher inclinations from this range: $i_{\text{xray}} \sim 55 - 65^\circ$. This implies that the inner accretion flow that generates most X-ray photons is viewed more edge-on than the binary orbit if the binary orbit is inclined at $i_{\text{orb}} \sim 30^\circ$. The corresponding misalignment angle of $\theta_{\text{BH}} \sim 15 - 35^\circ$ (or more likely of $\theta_{\text{BH}} \sim 25 - 35^\circ$) needs to be taken into account while modeling X-ray emission from Cyg X-1.

There are alternative explanations for high degree of polarization that do not require misalignment of accretion flow from the orbital plane. For example, the photosphere/corona is moving with mildly relativistic velocities (Poutanen et al. 2023; Dexter & Begelman 2023) or electrons and ions are distributed anisotropically in the photosphere/corona (Krawczynski et al. 2023).

And there is another interesting measurement from long-based (up to ~ 26 yr) multi-band radio observations indicating that orbit inclination is in fact $i_{\text{orb}} \sim 30^\circ$ with BH spin (jet axis) inclined at similar angle $i_{\text{xray}} = 31_{-3}^{+4}$ deg (an assumption is made that the inner accretion flow is aligned with BH spin plane) to the line of sight, but with BH spin axis misaligned with binary angular momentum by $\theta_{\text{BH}} = 22_{-6}^{+11}$ deg (Zdziarski et al. 2023b). Note that this imposes a very special spatial position of binary angular momentum and BH spin momentum vectors in respect to the observer.

8.3.2. The origin of the misaligned accretion flow

The most natural explanation for the misaligned accretion flow is to have BH with a spin vector misaligned with a binary angular momentum vector. This leads to the warped disk geometry, with outer disk parts aligned with the orbital plane and the inner parts of the disk aligned with the BH spin equatorial plane. Such configuration is caused by effects of the Lense-Thirring effect and the disk’s viscosity that makes the disk’s inner parts align with BH angular momentum (Bardeen & Petterson 1975). Required BH spin misalignment for such a scenario was reported for at least two BH systems. GRO J1655-40 is a system with BH spin misaligned by $\theta_{\text{BH}} \sim 15^\circ$ from binary angular momentum (MacCarone 2002; Martin et al. 2008), while BH misalignment angle in MAXI J1820+070 is $\theta_{\text{BH}} \gtrsim 40^\circ$ (Poutanen et al. 2022).

We work under the conservative assumption that both stars in Cyg X-1 had spins aligned with binary angular momentum vectors just before the BH formation. In such a case, the only process that could misalign BH spin is a natal kick at BH formation. Given the large size of Cyg X-1 orbit and a relatively short time since BH formation ($\lesssim 1.4$ Myr; see below) it is not expected that BH spin would realign with binary angular momentum (King & Nixon 2016, 2018; King 2023). The O star in Cyg X-1 is now close to the end of its main sequence and has a current mass of $M_{\text{O}} \approx 40 M_{\odot}$. Using MESA (Paxton et al. 2015) models we find that star with initial mass of $M_{\text{ZAMS}} = 60 M_{\odot}$ finished main-sequence that lasted ~ 4 Myr with mass of $\sim 40 M_{\odot}$. To get an upper limit on BH lifetime, we use a very massive star as a progenitor of BH so the BH formation happens as early as possible in the system’s history. The entire lifetime of a star with an initial mass of $M_{\text{ZAMS}} = 200 M_{\odot}$ is ~ 2.6 Myr. Therefore, the time from BH formation is $\tau_{\text{BH,life}} \lesssim 1.4$ Myr.

Here, we investigate the natal kick needed to misalign BH in Cyg X-1. We want to find such a natal kick that would (i) produce desired BH misalignment ($\theta_{\text{BH}} = 15^\circ$ or $\theta_{\text{BH}} = 25^\circ$ to probe polarization measurements) and that would (ii) result in the smallest increase of the systemic velocity. The latter is guided by the acclaimed origin of Cyg X-1 from Cyg OB3 O/B massive star association. The association (2.0 ± 0.3 kpc) and Cyg X-1 (2.22 ± 0.18 kpc) are found at similar distances and positions in the sky and apparent small relative velocity of Cyg X-1 with respect to the association ($V_{\text{rel}} = 10.7 \pm 2.7$ km s $^{-1}$; Mirabel & Rodrigues (2003); Rao et al. (2020)).

For a pre-BH formation system configuration similar to the current configuration ($M_1 = 21 M_{\odot}$: BH progenitor mass, $M_2 = 40 M_{\odot}$: companion star mass, $a = 52.5 R_{\odot}$, $e = 0.0$) we form BH with no mass loss and thus no associated Blaauw kick. However, we give BH a natal kick (i.e., its origin would come from the asymmetric neutrino emission). To obtain misalignment of $\theta = 15^\circ$ minimal natal kicks (in polar direction) of ~ 120 km s $^{-1}$ are required and they impart a systemic velocity of $V_{\text{sys}} \sim 42$ km s $^{-1}$. For misalignment angle of $\theta = 30^\circ$ minimal kicks are ~ 240 km s $^{-1}$ resulting in systemic velocity of $V_{\text{sys}} \sim 84$ km s $^{-1}$. Adding a Blaauw kick would only increase minimal systemic velocity for a

given required BH misalignment angle. These estimates are performed with the **StarTrack** code module, allowing for detailed calculations of various supernova geometries and kicks (Belczynski et al. 2008). Therefore, BH misalignment is achievable with moderate to large natal kicks, but it imparts systemic velocity significantly larger than the observed Cyg X-1 velocity.

At face value the above estimate disfavors BH spin misalignment in Cyg X-1 as inferred from polarization (Krawczynski et al. 2022) estimates as well as deduced from radio observations (Zdziarski et al. 2023b). This is if Cyg X-1 was born in the Cyg OB3 O/B association. However, Cyg X-1 is found at the very edge of the association, and it cannot be excluded that its position on the sky is just a chance (however small) coincidence.

Until now, we have ignored some observational data indicating that some binary systems may host stars with misaligned spins (Marcussen & Albrecht 2022). If it were true for Cyg X-1, a natal kick would not be needed to have a misaligned BH and small systemic velocity simultaneously. On the other hand, even if spins were aligned just before BH formation, there is a proposal of spin tossing at BH formation without imparting extra systemic velocity (Tauris 2022). Also, any dynamical encounters (e.g., fly-by or tertiary component present in the past) may have misaligned Cyg X-1 component spins.

From the perspective of our analysis for any of the proposed Cyg X-1 configuration, we have models of inner accretion flow, from low inclinations of $\sim 30^\circ$ (Sec. 5) to high inclinations of $\sim 60^\circ$ (this Section) that fit the best spectral data with low BH spins and thus do not create tension with LVK data.